Biochimica et Biophysica Acta 1837 (2014) 589–597

Contents lists available at ScienceDirect

Biochimica et Biophysica Acta

journal homepage: www.elsevier.com/locate/bbabio

Review

Ultrafast photochemistry of Anabaena Sensory Rhodopsin: Experiment and theory☆

Igor Schapiro [a,*], Sanford Ruhman [b,*]

[a] Max Planck Institute for Chemical Energy Conversion, Stiftstr. 34-36, 45470 Mülheim an der Ruhr, Germany
[b] Institute of Chemistry, The Hebrew University of Jerusalem, Jerusalem 91904, Israel

ARTICLE INFO

Article history:
Received 1 July 2013
Received in revised form 28 September 2013
Accepted 29 September 2013
Available online 5 October 2013

Keywords:
Anabaena Sensory Rhodopsin
Retinal chromophore
Photoisomerization
Photochromism
Time resolved spectroscopy
Excited state molecular dynamics

ABSTRACT

Light induced isomerization of the retinal chromophore activates biological function in all retinal protein (RP) driving processes such as ion-pumping, vertebrate vision and phototaxis in organisms as primitive as archea, or as complex as mammals. This process and its consecutive reactions have been the focus of experimental and theoretical research for decades. The aim of this review is to demonstrate how the experimental and theoretical research efforts can now be combined to reach a more comprehensive understanding of the excited state process on the molecular level. Using the Anabaena Sensory Rhodopsin as an example we will show how contemporary time-resolved spectroscopy and recently implemented excited state QM/MM methods consistently describe photochemistry in retinal proteins. This article is part of a Special Issue entitled: Retinal Proteins — You can teach an old dog new tricks.

1. Introduction

Light induced isomerization of the retinal chromophore activates biological function in all retinal protein (RP) driving processes such as ion-pumping, vertebrate vision and phototaxis in organisms as primitive as archea, or as complex as mammals [1,2]. The photoisomerization is not only ultrafast (it takes place on the femto- to picosecond time scale) but is also efficient [3,4], making it an archetype for conversion from solar to chemical energy on the molecular level. A detailed understanding of the mechanism of primary events in the various RPs, and how nature has optimized this reaction in the protein environment is not only of fundamental importance, but might also inspire technological advances in harnessing solar energy. Therefore this process and the photo-cycles it unleashes have been the focus of experimental and theoretical research for decades.

In this review, we begin by outlining milestones in experimental and theoretical research of electronic transitions in retinal proteins. The emphasis is placed on ultrafast processes, meaning on the initial step of photochemistry which deals with light absorption, excited state reactivity, and internal conversion (IC) to form the initial ground state photo-cycle intermediates. Until recently direct comparison between experiment and theoretical simulations has been hampered by inherent limitations of both approaches. The aim of this review is to demonstrate how the experimental and theoretical research efforts can now be combined to reach a more comprehensive understanding of the excited state process on the molecular level. Using the Anabaena Sensory Rhodopsin as an example we will show how contemporary time-resolved spectroscopy and recently implemented excited state QM/MM methods consistently describe photochemistry in RPs.

2. Experimental milestones

The ultrafast nature of retinal protein photochemistry was established early on using picosecond spectroscopy [5–7]. Those ground breaking pump-probe experiments concentrated on the familiar microbial and visual pigments — bacteriorhodopsin (BR) and bovine rhodopsin (RH). Just how rapid these transformations are was clarified in a series of pioneering experiments by Shank and Mathies, which were conducted with what was then revolutionary time resolution [8–10]. Those investigations demonstrated distinct differences between BR and RH photochemistry. Photoisomerization in bovine RH, completed within a remarkable 200 fs, exhibited continuous spectral evolution during the course of internal conversion which gives way to coherent vibrational wave packet motions in the primary photoproducts. In contrast, photoisomerization in BR was found to take nearly 3 times longer, with well defined excited state absorption and emission bands, and no such product coherences.

Ultrafast photochemical experiments have since tried to learn more about the causes and significance of these findings. To understand

Abbreviations: RPSB, Retinal protonated Schiff base; RP, Retinal protein; MRP, Microbial retinal protein; BR, Bacteriorhodopsin; RH, Bovine rhodopsin; ASR, Anabaena Sensory Rhodopsin

☆ This article is part of a Special Issue entitled: Retinal Proteins — You can teach an old dog new tricks.

* Corresponding author.
E-mail addresses: igor.schapiro@cec.mpg.de (I. Schapiro), sandy@mail.huji.ac.il (S. Ruhman).

0005-2728/$ – see front matter © 2013 Published by Elsevier B.V.
http://dx.doi.org/10.1016/j.bbabio.2013.09.014

which degrees of freedom in the retinal and/or the protein direct the photochemistry, and determine its speed and quantum efficiency. Two main themes underlie this effort — investigating the effects of controlled perturbations on the photochemistry, and direct probing of structural evolution while it is taking place. The latter has been attempted via methods of transient vibrational spectroscopy, and has provided some mode specific information concerning the course of photochemistry [11–16]. A full multi-mode perspective on retinal protein photochemistry has still yet to be obtained. Structural perturbations can be achieved by point mutations to the protein matrix [17–19], or by replacing the native retinal with artificial chromophores [20,21]. Work with point mutations has identified crucial residues within the protein whose interaction with the RPSB strongly affects photochemical dynamics as well as later photo-cycle events. Artificial pigment studies have highlighted the protein conferred bond selectivity of isomerization in MRPs. The protein environment can be further altered from native physiological conditions by changing pH, ionic strengths, temperature etc [22,23]. Comparing photochemical dynamics in the numerous microbial rhodopsin proteins (MRPs), identified since the discovery of BR, has also contributed to gaining insight concerning the questions posed above. This comparison has shown that isomerization rates vary significantly from one MRP to another, and are not simply correlated with protein induced spectral tuning or with the subsequent quantum efficiency of isomerization [24–29].

Perturbations have also been applied to primary events in RPs via multi-pulse sequences, which interrogate the reacting proteins during the course of photoisomerization [30–33]. Photochemistry in visual pigments is far less understood. Difficulties in their purification and manipulation have curtailed an equivalent approach to type II RPs, with only bovine RH photochemistry having been probed in detail on ultrafast timescales [8,9,34]. In the case of RH, naturally occurring retinal conformations have provided an alternative vehicle for probing structural effects on the course of photochemistry. Aside from the prevalent 11-*cis* reactant state of RH, the protein pocket can also accommodate a 9-*cis* retinal protonated Schiff base (RPSB) (Isorhodopsin). Upon excitation this variant is likewise transformed to all-*trans* but with reduced quantum yield. Photoisomerization rates measured with femtosecond spectroscopy are markedly reduced relative to internal conversion in RH. These two observations led to early suggestions that reaction rates and quantum efficiencies are correlated in RPs [35]. While scrutiny of all RPs has disproved this suggestion, more recent investigations of Isorhodopsin and RH may explain both effects in terms of bifurcation in the excited state into reactive and non-reactive pathways, with a branching ratio which strongly depends on the initial retinal configuration.

Here we take a similar approach to MRP photochemistry. Anabaena Sensory Rhodopsin is an MRP discovered in fresh water blue bacteria, which exhibits unique photo-switching properties. It exists in two stable ground state forms, one which contains an all-*trans*, and the other a 13-*cis* retinal moiety. Reactive photochemical events all cause the interchanging of ASR between these resting states. Relevant to our study is the fact that two naturally occurring and distinguishable S_0 reactant states are accessible in this protein. As in the case of Isorhodopsin, this allows an appreciation of how the initial retinal configuration influences the course of photochemistry in the same protein environment. As shown below the change in initial structure of the retinal alters the rates of IC momentously. Interpreting this by comparing our findings with recent QM/MM simulations of both reaction paths is the essence of our report.

3. Theoretical milestones

The theoretical work on RPs has a history as long as the spectroscopic studies. In 1976, in a seminal computational study on RH, Warshel proposed a space-saving retinal photoisomerization mechanism, requiring minor rearrangements in the retinal cavity [36]. In a so-called "bicycle-pedal" mechanism two double bonds rotate concertedly in opposite directions, such that the overall conformational change is minimized. The quantum-mechanical consistent force field method for pi-electron systems (QCFF/PI) has been used to compute the excited state potential energy surface of retinal during the molecular dynamics simulations. Steric interactions with the protein matrix have been modeled by a simple restraint on the retinal atoms. Since then, Warshel and his co-workers have successively improved the model, employing better structural data and new computational algorithms [37,38]. In their most recent work, Warshel and Chu [39] have used an advanced QM/MM setup, with improved Empirical Valence Bond (EVB) parameters for the excited state potential of the retinal chromophore and introducing polarization of the protein environment by the QM atoms. Using this methodology multiple excited state simulations of the photoisomerization in bacteriorhodopsin have been performed based on a high-resolution X-ray structure. Warshel and coworkers finally arrived to the conclusion of an aborted bicycle-pedal mechanism in RPs which is characterized by simultaneous rotation of two double bonds, one of which is completed successfully while the other one is aborted. However, this pioneering work has inspired many researchers to propose alternative mechanisms which could explain the space-saving and ultrafast photoisomerization of retinal in the protein. In the so called "hula-twist" mechanism by Liu et al. the isomerization of neighboring single and double bonds at the same time was proposed to achieve a volume-conserving motion in the protein pocket [40–42]. Another example is a mechanism reminiscent of the crankshaft motion that was extracted from RH [43] QM/MM simulations. This mechanism is also called an asynchronous bicycle pedal isomerization since the different bond rotations are not concerted. More recently, a "double bicycle-pedal" [44] or "folding-table" [45] mechanism was proposed for BR.

The first ab initio QM/MM simulation of retinal's photoisomerization in the protein environment has been reported by Schulten and coworkers for bacteriorhodopsin in 2003 [46]. A small part of the retinal, from C11 to Cε, was described at the CASSCF level of theory. All π-electrons and orbitals were included in the active space of the truncated chromophore, that resulted in six electrons in six orbitals. The remaining atoms of the retinal chromophore together with the protein were calculated with an Amber [47] force-field. In 2004 a QM/MM study of RH was conducted by the Rothlisberger group [48]. The model was built on the basis of the crystal structure of bovine RH from Teller et al. [49] and embedded in a membrane environment. Density functional theory was used to describe the RPSB, in particular the restricted open-shell Kohn–Sham (ROKS) method was employed in the excited state. Based on two QM/MM trajectories at different temperatures and 25 classical trajectories, where the photoisomerization was induced by inverting the torsional potential, the authors made conclusions about the mechanism of the photoprocess. It was confirmed that the protein pretwists the chromophore around C11 – C12 and therefore selects this bond for isomerization. Further, the simulations revealed the isomerization to occur under minor displacements of the retinal backbone leading to a highly strained geometry. This intramolecular strain together with the increase in steric interaction energy with the protein binding pocket explained the storage of the photon energy.

A few years later Olivucci's group succeeded for the first time to treat the full retinal chromophore at the CASSCF level of theory. In this significant computational effort, an excited state QM/MM molecular dynamics simulation of 11-*cis*-retinal in bovine rhodopsin was performed [43]. The full π-system of the chromophore was included in the active space, which comprised 12 electrons in 12 orbitals. To compensate for the lack of dynamic electron correlation, the forces that were evaluated on-the-fly at the CASSCF level were scaled linearly to match the forces obtained at the CASPT2 level of theory. This approximation was validated by comparing CASSCF and CASPT2 energies along a relaxed scan. The authors found that only the steepness was different between the energy profiles described at these two levels.

Therefore a linear scaling of the gradient was a good approximation to account for the dynamic electron correlation in an empirical manner. Furthermore a relation was derived which showed that gradient scaling is equivalent to the scaling of the time step in the molecular dynamics simulation. Hence, the so called scaled-CASSCF trajectory was obtained. The protein was described by an extension of the Amber force field, in which charges on the atoms in the vicinity of the retinal were reparameterized [50]. Using this advanced setup the authors were able to reproduce the experimentally determined excited state lifetime of 100 fs. In 2009 Hayashi et al. [51] have applied a similar QM/MM approach with a slightly more truncated model chromophore. In total 14 trajectories were calculated at the CASSCF/AMBER level of theory. All of them were found to decay to the ground state within 100 fs which is of the same order of magnitude as the trajectory by Frutos et al. [43]. Bathorhodopsin is formed in 13 cases and in one case a 9-*cis* isomer (Isorhodopsin) is produced by a bicycle pedal isomerization of C9═C10 and C11═C12 bonds, as originally proposed by Warshel [36]. A similar result was found for a set of gas phase trajectories where the concerted isomerization of two double bonds was a rare event [52]. However, an accompanying rotation of 60°, on average, is found around C9═C10 in the 13 trajectories showing an aborted bicycle pedal-type mechanism, which is consistent with the previous findings. An even larger set, namely 38 trajectories, was used to generate a differential transition map which was in qualitative agreement with the timed resolved spectroscopy in a joined computational and experimental work [34].

In a comparison of the excited state dynamics of RH and Isorhodopsin by Ishida and coworkers, the slower isomerization of the 9-*cis* isomer in the protein has been successfully reproduced [53]. RH was found to undergo a ballistic decay to the ground state while Isorhodopsin was found to approach the conical intersection several times before the return to the ground state. Steric hindrance induced by the protein specifically in the vicinity of the C9═C10 double bond has been determined as a reason for the different excited state reactivity. Further molecular dynamics investigations were carried out on Bathorhodopsin, the first isolatable intermediate of RH. In the first computational study by Birge et al. [54] semiempirical methods were used to perform molecular dynamics simulations. The highly twisted retinal in Bathorhodopsin was found to isomerize faster than the 11-*cis* analog in RH. In a more recent study QM/MM simulations have shown that Bathorhodopsin reaches the conical intersection in 50 fs which is nearly twice as fast as RH [55].

The effect of the protein environment on the photoisomerization of RPSB was studied in detail by the Martinez group [56]. In order to evaluate the role of the protein, the RPSB was also calculated in the gas phase as well as the methanol solution. The excited state dynamics simulations revealed the decay to the ground state being faster in the gas phase as compared to the protein and significantly slower in methanol solution. However, the all-trans RPSB was found to be the dominant product in RH, while the isomerization was aborted in the gas phase as well as methanol solution, leading back to the 11-*cis* isomer.

The simulations mentioned above have provided atomistic insights into the sequence of events initiated by photon absorption. Overall they contributed to a general mechanism where immediately after excitation to S_1, bond-length relaxation takes place that occurs on a time scale of 10–30 fs. This initial relaxation phase is followed by a space-saving isomerization process that includes a major torsion of the isomerizing bond, accompanied by partial twist of bonds in the vicinity to reduce the space required for the isomerization. Selectivity is achieved by steric interactions that hinder full rotations around other bonds. Furthermore, the chromophore is rapidly channeled by the protein environment towards the seam region in contrast to the situation in solution.

4. Anabaena Sensory Rhodopsin

ASR was discovered nearly a decade ago in the genome of the *Anabaena* (*Nostoc*) sp. PCC7120 cyanobacterium [57]. Although the biological role of ASR is still under investigation [58–62], it most likely serves as a sensory photoreceptor, making it the first sensory rhodopsin discovered in bacteria. This is also based on the fact that the abundance of both stable ground state forms is determined by the wavelength and intensity of ambient light. The ASR protein is co-expressed with a cytoplasmic transducer protein (ASRT) which discriminates between the two configurations, and in turn attaches to DNA presumably to regulate gene expression. Assigning a sensory role to ASR is also based on the finding that its photochemistry is purely photoswitching [63,64]. In other words, once photoisomerization has occurred, the ultimate product is the opposite switching state. The stable resting states of the retinal moiety are identical in ASR and in dark adapted (DA) BR: 13-*cis*, 15-*syn*, (13C) and all-*trans*, 15-*anti* (AT). In ASR irradiation actually enhances coexistence of both forms. This situation is unlike that for BR where regardless of the initial state, the ultimate product of repeated photoexcitation is all-*trans* [65,66].

The existence of two reversible half-cycles starting either from 13C or AT (Fig. 1), both of which are functionally relevant under physiological conditions, makes ASR photochemistry particularly interesting. The mechanisms underlying the differences in photochemical dynamics between visual pigments and microbial RPs remain the subject of debate. One possibility is that these differences stem from the retinal photoisomerization coordinate active in each case, all-*trans* to 13-*cis* in the microbial proteins vs. 11-*cis* to all-*trans* for the visual pigments. While this is probably not the only factor which determines the differences in photochemical dynamics of type I and type II RPs, for isolating the effect of changing the initial configuration one might probe photoisomerization dynamics in a retinal protein which naturally accommodates both all-*trans* and *cis* configurations.

Structural studies on ASR to date did not indicate significantly twisted conformations in either of the switching states (although X-ray studies did not perfectly separate the two isomers) [59]. Thus, the significance of studying excited state dynamics for both initial states in ASR is (a) Revealing the effect that *cis* vs all-*trans* initial configuration has on the course of photochemistry within the protein, and (b) Providing, along with structural data, valuable inputs for comparison with advanced quantum chemical simulations. The fact that both processes take place in the same protein surroundings can narrow uncertainties experienced when comparing "opsin effects" in different RPs, making ASR a unique test case.

5. Spectroscopy

5.1. Hyperspectral pump-probe experiments on ASR

In view of the above expectations, the course of IC in ASR was recorded by multichannel detection methods covering the range from 450 to 1500 nm with sub-100 femtosecond temporal resolution [67]. Excitation and probing pulses were derived from an amplified Ti:Sapphire laser system. Pump pulses were obtained from an optical parametric amplifier (TOPAS, Light Conversion), and probe from supercontinuum generated in sapphire. An intensity spectrum of the pump pulse is included with the pigment spectra in Fig. 2. Visible to NIR hyperspectral detection was performed on silicon and InGaAs diode array spectrographs as described in detail elsewhere.

Experiments were conducted for two ASR samples. The first dark adapted (DA) sample was kept in the dark overnight. The other was light-adapted (LA) by continuous irradiation with orange light. HPLC measurements confirmed that the former was nearly 100% AT, while the latter was more than 65% 13C. A color coded map of pump induced changes in absorption from photo-excited DA–ASR, corresponding to all-*trans* ASR (ASRAT), is shown in panel A of Fig. 3. It exhibits trends reminiscent of other microbial RPs — a bleach band near the ground state absorption maximum, and short lived excited state absorption and emission bands centered at ~500 and ~900 nm respectively. Following the decay of these bands, a permanent residual difference signal

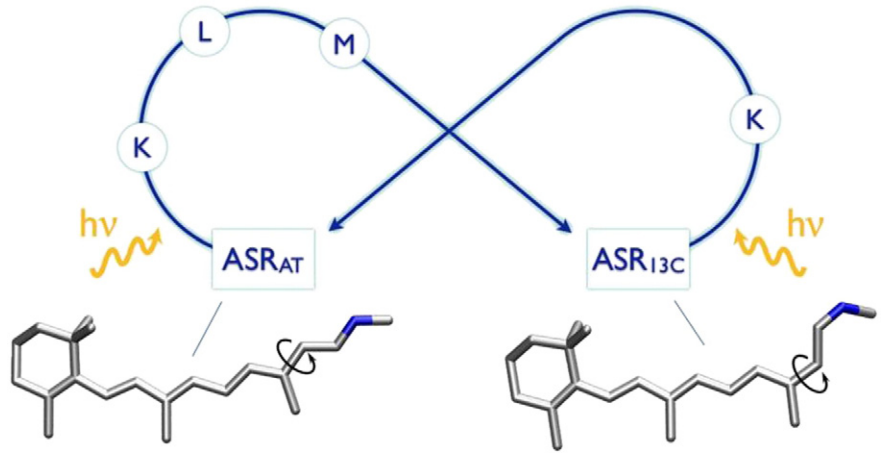

Fig. 1. Photoisomerization in Anabaena Sensory Rhodopsin. The two photocycles convert the all-*trans* and the 13-*cis* RPSB isomers into each other via the intermediates K, L, M.

due to photoproducts is apparent. These trends are highlighted in spectral cuts positioned at the peaks of excited state absorption and emission, as well as that of the ground state bleach, in panel C.

Kinetic analysis of the two data sets obtained demonstrated that after ~0.5 ps, the transient spectra in both were identical within a constant multiplicative factor. Since the dark adapted sample contains only all-*trans* ASR, this convergence shows that at longer delays only excited AT–ASR remains even when exciting the light adapted sample. The relative intensities of the transient spectra in this convergent state were also shown to be consistent with the known isomer ratios in the light adapted sample. Using the relative intensities of signal at long times, a subtraction of AT–ASR contributions to light adapted sample transient spectra was conducted to extract a pure 13C–ASR signal.

A similar mapping of the results of this subtraction is presented in panel B of Fig. 3. Along with analogous spectral cuts presented alongside those from AT–ASR in panel C as well, this map demonstrates remarkably rapid IC in the 13C reactant state, which is virtually over in ~250 fs — nearly an order of magnitude faster than the opposite process. This wide disparity in rates is surprising, since no signs of drastic crowding and/or pre-twisting of the retinal, implicated in rapid IC of the visual pigments, have been detected in either resting state of the ASR. It is important to point out that the route of lesser quantum yield actually undergoes IC much faster. While the photochemistry of ASR is 100% photo-switching, the efficiency of an absorbed photon to actually promote reaction is relatively low for both resting states, ~40% for all-*trans*, 15-*anti*, and only ~12% for the 13-*cis*, 15-*syn*. This provides yet another indication that quantum yields and IC rates are not generally correlated in MRPs.

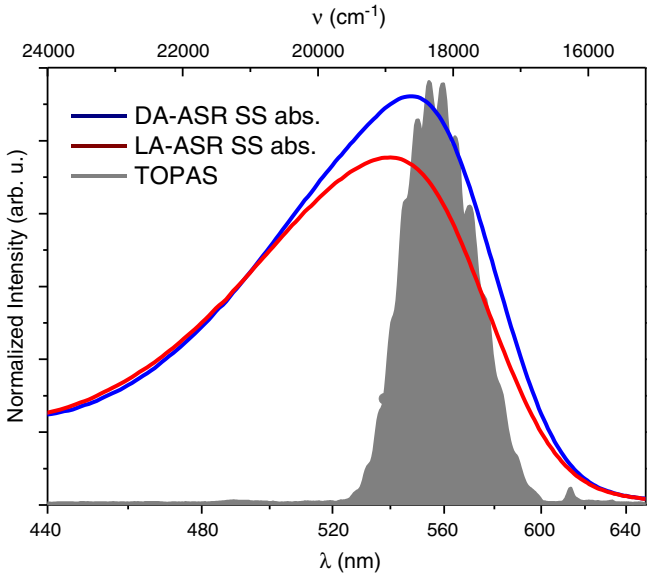

Fig. 2. Spectra of light and dark adapted samples of ASR along with the spectrum of the OPA pulses used as pump.

5.2. QM/MM simulation

The first crystal structure of ASR [59] provided the basis for a QM/MM model used as a starting point for simulations by Strambi et al. [68] in 2010. A previously established QM/MM protocol employed in that study is based on ab initio multiconfigurational theory which was shown to provide RP structures and excitation energies consistent with the experimental data [50,69,70]. For instance, using a CASPT2//CASSCF/6-31G*/AMBER protocol it was shown that it is possible to construct an accurate RH model [70]. The computational details of the CASPT2//CASSCF/6-31G*/AMBER protocol are fully described in Ref. [71]. Briefly, the QM/MM partitioning is defined by truncating the $C_\delta - C_\varepsilon$ bond of the Lys210 side chain and capping the quantum mechanical (QM) region with a hydrogen link atom (Fig. 4). Hence, the QM region which is described at multiconfigurational level of theory contains the full retinal including the protonated Schiff base bond up to the C_ε atom. The active space in the CASSCF calculation comprises the full π-system of the retinal (12 electrons in 12 π-type orbitals). In order to account for the interaction of the QM and the MM regions the electrostatic embedding scheme is used. The AMBER force field describes the protein and charges included therein account for the polarization effects in a mean-field way. The computation was carried out using the MOLCAS [72,73] quantum chemistry program in conjunction with the Tinker [74] molecular mechanics program.

In the work by Strambi [68] the absorption spectra of both the all-*trans* and 13-*cis* isomers in ASR were reproduced quantitatively by the QM/MM protocol. The same models provided the basis for the investigation of the light-driven steps of the photochromic cycle. For this purpose minimum energy paths (MEPs) were calculated in the excited state (S_1) starting from the ASRAT and ASR13C models yielding the primary photoproducts (ASRAT–K and ASR13C–K). These MEPs connect the Franck–Condon points on S_1 to the points where decay to the ground state (S_0) occurs. As shown in Fig. 5, consistently with what was already observed for RH [70,75], both paths lead to a S_1/S_0 conical intersection (ASRAT–CI and ASR13C–CI, respectively) where the S_0 and S_1 potential energy surfaces cross and the decay probability is expected to be high. Starting from 13° twisted ASRAT and ASR13C structures the conical intersection was reached before 90° of twisting

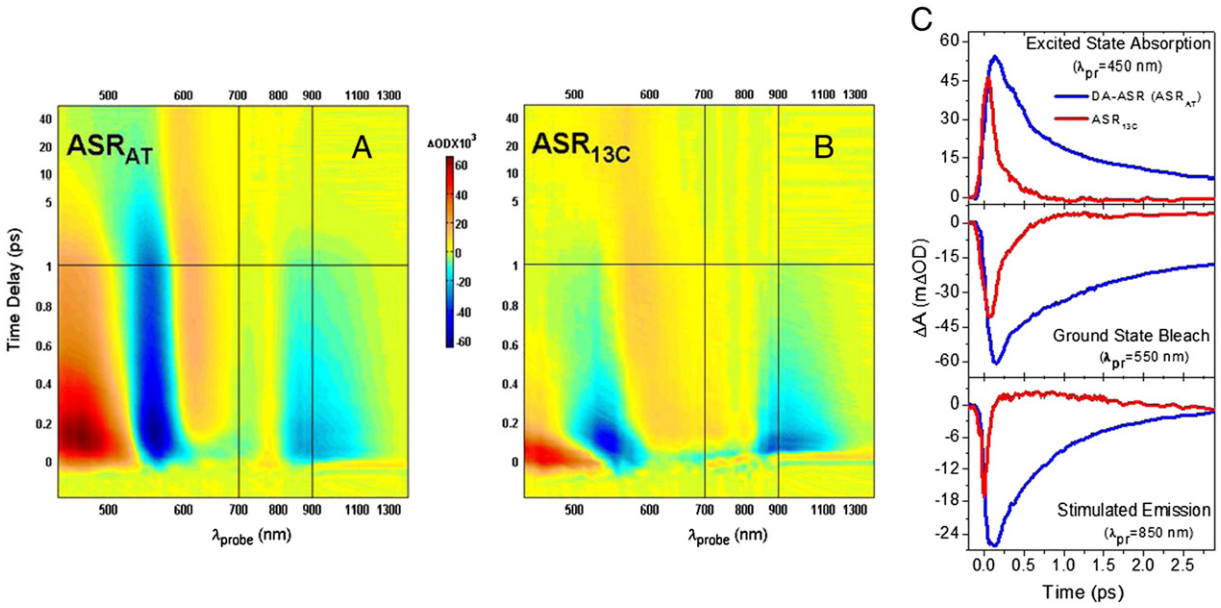

Fig. 3. Color coded mapping of transient absorption data for AT (panel A) and 13C–ASR (panel B). The extreme shortening internal conversion for the latter can be seen both in these maps and in the cuts at selected wavelengths depicted in panel C.

with C13=C14 angles of −108° and +84°, respectively. Analysis of the geometrical changes along the photoisomerization of the all-*trans* and 13-*cis* retinal chromophores revealed a unidirectional, counterclockwise 180° rotation with respect to the Lys210-linkage of the chromophore axis. Thus, it was concluded that the sequential interconversions of the all-*trans* and 13-*cis* forms during a single photochromic cycle yield a complete (360°) unidirectional rotation. This finding implies that ASR is a biological realization of a light-driven molecular rotor. Recently, also the effect of protein mutations on spectroscopic properties in ASR was studied computationally by Melaccio et al. [80] The computed absorption maxima spanned an 80 nm range and their variation was explained with the electrostatic effects induced by the protein cavity onto the chromophore.

Starting from the ASR models by Strambi et al. excited state QM/MM trajectories were computed. The CASSCF method was used to describe the ground and the excited state of RPSB. Two roots with equal weights were included in the state averaged CASSCF wavefunction. A set of coupled perturbed CASSCF equations was solved, using the multiconfigurational linear response theory [76], in order to obtain the state specific orbital coefficients. These corrected molecular orbital coefficients were used for the analytic gradient calculation. The same 6-31G* basis set was used for consistency and comparison with previous work on RPs. The velocity Verlet algorithm and forces obtained from the same QM/MM setup were used to propagate Newton's equation of motions. Once the S_1 and S_0 state potentials approach, a surface hopping algorithm [77–79] was employed to detect transitions between the

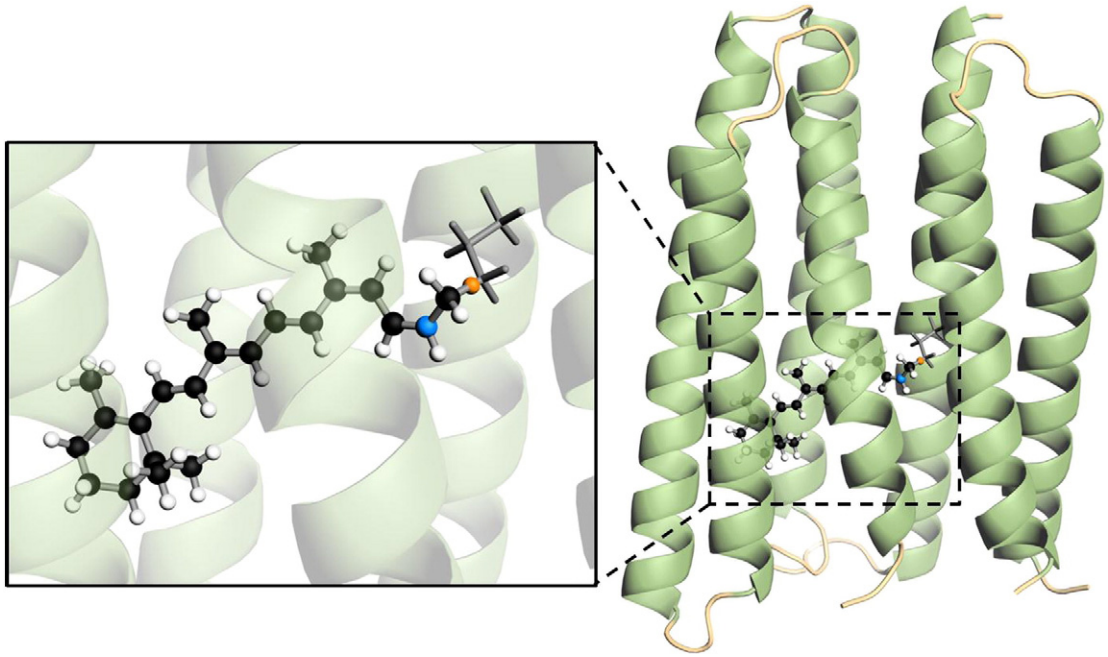

Fig. 4. The QM/MM model of ASR13C. The protein is shown in the cartoon representation. The QM region contains the protonated retinal Schiff base up to the C_ε atom, shown in ball-and-stick representation with color-coded atoms. The MM part of the lysine sidechain is shown in the stick representation and colored in gray. A link atom (colored in orange) is placed at the boundary between the QM and the MM region.

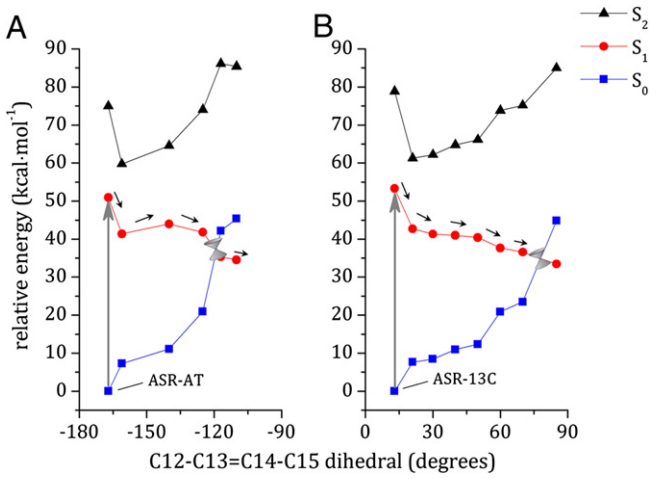

Fig. 5. CASPT2//CASSCF/AMBER energy profiles along the S_1 photoisomerization path of ASRAT (A) and ASR13C (B). S_0 and S_2 energy profiles along the S_1 path are also given. The S_1 path is computed in terms of a relaxed scan along the reactive C12–C13═C14–C15 dihedral angle. The location of the conical intersection ASRAT–CI is revealed by the change in the character of the S_1 electronic state. Data plotted from reference [68].

states. Due to the high computational demands of these calculations only single trajectories for each isomer of ASR were computed. A simulation of 50 to 70 time step takes one month of computer time on a modern supercomputer facility. Hence, the molecular dynamics simulations were carried out for one trajectory starting without initial kinetic energy from the optimized ground state minimum. In a previous work on RH by Frutos et al. [43] it was shown that these so-called 0 K-trajectories (which are trajectories starting from the optimized ground state geometry with zero initial velocity) propagate in the center of a wavepacket, hence mimicking an ensemble of trajectories. Hence they can be used for mechanistic and stereochemical description.

The QM/MM semi-classical trajectories for ASR13C and ASRAT were calculated from the ground state minimum that also served as a starting point of the minimum energy path calculations by Strambi et al. [68]. Starting from the FC region on the S_1 potential energy surface (Fig. 6) the 13C trajectory is found to reach the conical intersection within 150 fs. As previously reported for RH [55] the initial relaxation is dominated by two reaction coordinates in sequence. Firstly, the pattern of alternating single and double bonds is completely inverted. The panel at the bottom of Fig. 6 demonstrates this so called inversion of the bond length order for the double bond C13═C14 and the single bond C12–C13. Within 20 fs the elongation of the C13═C14 bond makes it essentially a single bond. At the same time the C12–C13 single bond is significantly contracted to a double bond. This weakening of the bond prepares the isomerizing bond for rotation, which is subsequently the second reaction coordinate. In consequence the C–C13═C14–C dihedral undergoes a rotation that guides the chromophore to the conical intersection where the S_0 and the S_1 states are becoming degenerate. The previously published stereochemical rules for RH and Bathorhodopsin can be applied here to understand how small changes can determine the outcome of the reaction after the relaxation to the ground state mediated through the conical intersection. In contrast the trajectory of ASRAT is not undergoing the same evolution in over 400 fs of the simulation time. The present status of the simulation points to a significantly longer time scale of the photoisomerization than for ASR13C. This is in line with recent time-resolved experiments [67] reported in the "Spectroscopy" section above which find the isomerization of ASRAT to be at least one order of magnitude slower than in ASR13C. The analysis of the trajectory obtained so far shows that the bond length alternation has been inverted already. Hence the stretched double bond should allow the rotation to take place. But the torsion of the isomerizing double bond deviates only by less than 30° from the planarity which can be attributed to the presence of an excited state barrier. After the passage of the barrier a conical intersection can be reached as in the case of the ASR13C. The origin of the barrier for one distinct isomer is still unknown and requires more detailed characterization of the excited state potential. However, the occurrence of the barrier for the ASRAT confirms that an initial pretwisting of the retinal chromophore on the ground state is not responsible for the longer excited state lifetime.

5.3. Experiment vs theory

The results of the independently conducted experimental and theoretical studies can be complemented to get a more detailed picture

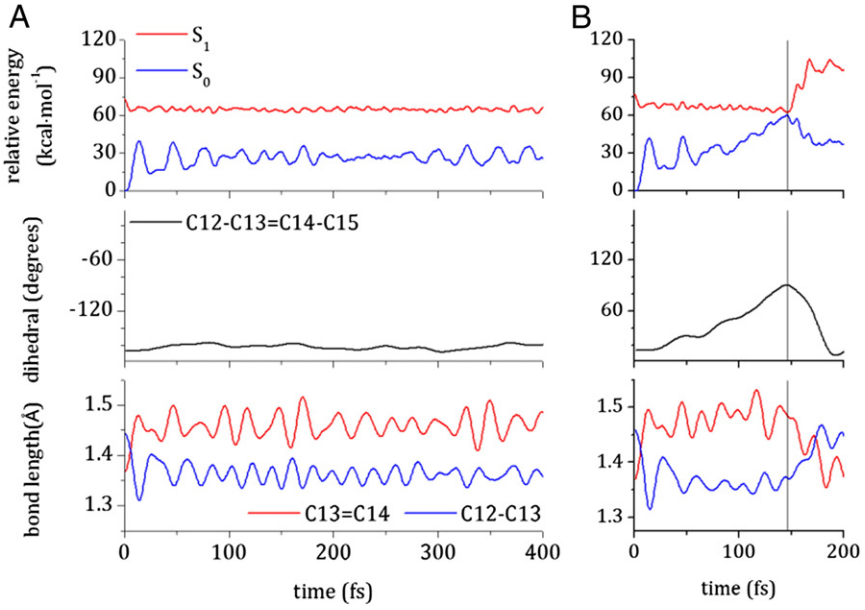

Fig. 6. QM/MM trajectories of ASR–AT (panel A) and ASR–13C (panel B). The top panels show the evolution of the ground and excited energies at the CASSCF(12,12)/6-31G* level of theory. The middle panels contain the torsion of the C12–C13═C14–C15 dihedral angle. The panels on the bottom depict the typical evolution of a single and a double, in this case C12–C13 and C13═C14. In the figures of the ASR13C models the vertical, dotted line indicates the time of the hop.

of the molecular rearrangements and mechanisms of the photoisomerization in ASR. In this section the limits in agreement between experiment and theory are discussed. The significance of the comparison of the two reactive channels in an identical protein environment is later reiterated. Finally we provide an outlook on further work that will lead to a better understanding of the primary photochemistry in ASR. In contrast to most previous studies on the photoisomerization of RPs the excited state molecular dynamics study was conducted as the experimental investigation was under way, and in ignorance of the ultrafast spectroscopic findings. The results of QM/MM minimum energy paths calculations by Strambi et al. [68] were published nearly one year ahead the experimental work, providing the first insight into the initial photochemistry of ASR. These simulations have determined the photoisomerization in ASR to be a unidirectional rotation. On the basis of these calculations a full two stage photo-cycle in ASR is predicted to comprise a full clockwise rotation of 360°, an aspect which has yet to be demonstrated experimentally. This might be made possible using a time resolved spectroscopic method that can distinguish between the two different rotational senses in the protein environment, such as circular dichroism UV or IR spectroscopy.

Nonetheless the static calculations by Strambi et al. [68] do not provide information about the excited state lifetimes and the quantum yields. A computational study of these properties requires an explicit consideration of the kinetic energy which is not included in this type of simulations. A first step in this direction was taken by excited state molecular dynamics simulations described above. These simulations track the photo-reaction in time, therefore allowing for a correlation of structural rearrangements in the time domain that can be compared to those obtained from transient spectroscopy. These trajectories were started from the same QM/MM model as in the minimum energy paths calculations. The trajectory starting from ASRAT was found to remain on the excited state for the simulation time of 400 fs (Fig. 6A). Even after this considerable delay, the trajectory has remained on the excited state and is still in progress. The experimental probability to find a trajectory in the excited state 400 fs after excitation of the AT–ASR is higher than 60% [67].

In contrast, the ASR13C trajectory was found to have an excited state residence time of 150 fs (Fig. 6B). Comparing this with the experimental results on probabilistic footing is more challenging. To begin with, the briefness of the ASR13C internal conversion is most likely limited by nuclear inertia, and should accordingly take place with markedly non-exponential dynamics, probably much closer to a Gaussian decay etc. This would imply an induction period for attaining the structure and nuclear momenta required for curve crossing. The 150 fs transit time simulated coincides almost perfectly with that predicted to be most probable based on a Gaussian fitting to the data of Wand et al. [67]. Agreement with experiment can also be seen the ASR13C trajectory reconstituting the initial resting state after the relaxation to the ground state. This is in line with the low quantum yield found for 13-*cis* to *trans* isomerization experimentally. While it is obvious that numerous trajectories will be required to establish the statistical significance of this good agreement, simulations of both ASR13C and ASRAT seem to be in line with experiment.

The results of excited state mapping by Strambi et al. [68] can be used to rationalize the longer excited state lifetime of ASRAT compared to ASR13C. Fig. 5 A shows the topology of the excited state potential energy surface of AT. A small barrier of only few kcal·mol^{-1} can be found between 150 and 130° of twist, in line with the molecular dynamics simulations. Interestingly a similar barrier for the 13C isomer is missing which may explain the significantly faster decay. However, it should be critically noted that for quantitative comparison a single trajectory of each isomer is not sufficient. Hence, the initial conditions have to be sampled to provide a basis for the simulation of a large set of trajectories from which statistical measures such as quantum yields and lifetimes can be deduced. Molecular dynamics simulations of this type are currently in progress.

On the experimental side the time resolved measurements by Wand et al. [67] were the first to characterize the ultrafast photoisomerization of both isomers. The major findings were that the ASRAT is at least 5 times slower than ASR13C but having a higher quantum yield. While analogous *cis* retinal isomers in VR and MR are known to have a shorter excited state lifetime than all-*trans* isomers, the missing link between the efficiency and the reaction speed was demonstrated for the first time in one single protein. From the experimental side a more detailed coverage of intermediate structures for both initial states is highly desirable. In the simulation the reactant is well-defined in contrast to the experiment where a mixture of the different isomers must be separated.

We conclude that a first step towards the understanding of the primary photochemistry in the ASR can be achieved by combining theory and experiment. The results of the molecular dynamics simulations are in semi-quantitative agreement with the observed differences between ASRAT and ASR13C excited state lifetimes. The fact that both the experimental and the computational studies were carried out independently suggests that QM/MM simulations have become of predictive power, allowing interpretation of detailed experimental data and in this case clarifying the factors affecting ASR photoreactivity. These simulations show that a barrier between 150° and 130° of the ASRAT, and not a pre-twisting and crowding of the chromophore, is responsible for the stark differences in reactivity of the two isomeric forms. However, further computational studies are on the way, including multiple trajectories starting from different initial conditions, to substantiate these findings with much higher statistical certainty.

Acknowledgement

This work was supported by the Israel Science Foundation, which is administered by the Israel Academy of Sciences and Humanities and US-Israel Binational Science Foundation. S.R. thanks Amir Wand, Rinat Rozin, and Mordechai Sheves for their collaboration on the experimental study of ASR. I.S. thanks Massimo Olivucci, Federico Melaccio and Alessio Valentini for the valuable discussions.

References

[1] J.L. Spudich, C. Yang, K. Jung, E.N. Spudich, Retinylidene proteins: structures and functions from archaea to humans, Annu. Rev. Cell Dev. Biol. 16 (2000) 365–392.
[2] J.L. Spudich, K. Jung, Microbial rhodopsins: phylogenetic and functional diversity; handbook of photosensory receptors, Wiley-VCH Verlag GmbH & Co. KGaA, 2005, pp. 1–23.
[3] U. Haupts, J. Tittor, D. Oesterhelt, Closing in on bacteriorhodopsin: progress in understanding the molecule, Annu. Rev. Biophys. Biomol. Struct. 28 (1999) 367–399.
[4] H.J.A. Dartnall, in: H.J.A. Dartnall (Ed.), Photosensitivity, Photochemistry of Vision Springer Verlag, Berlin, Heidelberg, New York, 1972, pp. 122–145.
[5] K.J. Kaufmann, P.M. Rentzepis, W. Stoeckenius, A. Lewis, Primary photochemical processes in bacteriorhodopsin, Biochem. Biophys. Res. Commun. 68 (1976) 1109–1115.
[6] E. Ippen, C. Shank, A. Lewis, M. Marcus, Subpicosecond spectroscopy of bacteriorhodopsin, Science 200 (1978) 1279–1281.
[7] B.H. Green, T.G. Monger, R.R. Alfano, B. Aton, R.H. Callender, Cis–trans isomerisation in rhodopsin occurs in picoseconds, Nature 269 (1977) 179–180.
[8] R.W. Schoenlein, L.A. Peteanu, R.A. Mathies, C.V. Shank, The first step in vision: femtosecond isomerization of rhodopsin, Science 254 (1991) 412–415.
[9] Q. Wang, R.W. Schoenlein, L.A. Peteanu, R.A. Mathies, C.V. Shank, Vibrationally coherent photochemistry in the femtosecond primary event of vision, Science 266 (1994) 422–424.
[10] R. Mathies, C. Brito Cruz, W. Pollard, C. Shank, Direct observation of the femtosecond excited-state cis–trans isomerization in bacteriorhodopsin, Science 240 (1988) 777–779.
[11] J. Herbst, K. Heyne, R. Diller, Femtosecond infrared spectroscopy of bacteriorhodopsin chromophore isomerization, Science 297 (2002) 822–825.
[12] T. Kobayashi, T. Saito, H. Ohtani, Real-time spectroscopy of transition states in bacteriorhodopsin during retinal isomerization, Nature 414 (2001) 531–534.
[13] L. Song, M. El-Sayed, Primary step in bacteriorhodopsin photosynthesis: bond stretch rather than angle twist of its retinal excited-state structure, J. Am. Chem. Soc. 120 (1998) 8889–8890.
[14] P. Kukura, D.W. McCamant, S. Yoon, D.B. Wandschneider, R.A. Mathies, Structural observation of the primary isomerization in vision with femtosecond-stimulated Raman, Science 310 (2005) 1006–1009.
[15] A. Kahan, O. Nahmias, N. Friedman, M. Sheves, S. Ruhman, Following photoinduced dynamics in bacteriorhodopsin with 7-fs impulsive vibrational spectroscopy, J. Am. Chem. Soc. 129 (2007) 537–546.

[16] G.I. Groma, A. Colonna, J. Martin, M. Vos, Vibrational motions associated with primary processes in bacteriorhodopsin studied by coherent infrared emission spectroscopy, Biophys. J. 100 (2011) 1578–1586.
[17] L. Song, M.A. El-Sayed, J.K. Lanyi, Protein catalysis of the retinal subpicosecond photoisomerization in the primary process of bacteriorhodopsin photosynthesis, Science 261 (1993) 891–894.
[18] S.L. Logunov, M. El-Sayed, J.K. Lanyi, Catalysis of the retinal subpicosecond photoisomerization process in acid purple bacteriorhodopsin and some bacteriorhodopsin mutants by chloride ions, Biophys. J. 71 (1996) 1545–1553.
[19] J. Briand, J. Léonard, S. Haacke, Ultrafast photo-induced reaction dynamics in bacteriorhodopsin and its Trp mutants, J. Opt. 12 (2010) 084004.
[20] A. Aharoni, B. Hou, N. Friedman, M. Ottolenghi, I. Rousso, S. Ruhman, M. Sheves, T. Ye, Q. Zhong, Non-isomerizable artificial pigments: implications for the primary light-induced events in bacteriorhodopsin, Biochem. Mosc. 66 (2001) 1210–1219.
[21] H. Kandori, H. Sasabe, K. Nakanishi, T. Yoshizawa, T. Mizukami, Y. Shichida, Real-time detection of 60-fs isomerization in a rhodopsin analog containing eight-membered-ring retinal, J. Am. Chem. Soc. 118 (1996) 1002–1005.
[22] M.A. El-Sayed, S. Logunov, On the molecular origin of the protein catalysis of the primary process in bacteriorhodopsin photosynthesis: retinal photoisomerization, IUPAC, Vol. 69, BLACKWELL SCIENCE LTD, P O BOX 88, OSNEY MEAD, OXFORD, OXON, ENGLAND OX2 0NE, 1997, pp. 749–754.
[23] S.L. Logunov, T.M. Masciangioli, V.F. Kamalov, M. El-Sayed, Low-temperature retinal photoisomerization dynamics in bacteriorhodopsin, J. Phys. Chem. B 102 (1998) 2303–2306.
[24] H. Kandori, K. Yoshihara, H. Tomioka, H. Sasabe, Primary photochemical events in halorhodopsin studied by subpicosecond time-resolved spectroscopy, J. Phys. Chem. 96 (1992) 6066–6071.
[25] T. Arlt, S. Schmidt, W. Zinth, U. Haupts, D. Oesterhelt, The initial reaction dynamics of the light-driven chloride pump halorhodopsin, Chem. Phys. Lett. 241 (1995) 559–565.
[26] F. Peters, J. Herbst, J. Tittor, D. Oesterhelt, R. Diller, Primary reaction dynamics of halorhodopsin, observed by sub-picosecond IR — vibrational spectroscopy, Chem. Phys. 323 (2006) 109–116.
[27] T. Nakamura, S. Takeuchi, M. Shibata, M. Demura, H. Kandori, T. Tahara, Ultrafast pump-probe study of the primary photoreaction process in pharaonis halorhodopsin: halide ion dependence and isomerization dynamics, J. Phys. Chem. B 112 (2008) 12795–12800.
[28] M.O. Lenz, R. Huber, B. Schmidt, P. Gilch, R. Kalmbach, M. Engelhard, J. Wachtveitl, First steps of retinal photoisomerization in proteorhodopsin, Biophys. J. 91 (2006) 255–262.
[29] I. Lutz, A. Sieg, A.A. Wegener, M. Engelhard, I. Boche, M. Otsuka, D. Oesterhelt, J. Wachtveitl, W. Zinth, Primary reactions of sensory rhodopsins, Proc. Natl. Acad. Sci. U. S. A. 98 (2001) 962–967.
[30] M. Yan, L. Rothberg, R. Callender, Femtosecond dynamics of rhodopsin photochemistry probed by a double pump spectroscopic approach, J. Phys. Chem. B 105 (2001) 856–859.
[31] S. Ruhman, B. Hou, N. Friedman, M. Ottolenghi, M. Sheves, Following evolution of bacteriorhodopsin in its reactive excited state via stimulated emission pumping, J. Am. Chem. Soc. 124 (2002) 8854–8858.
[32] O. Bismuth, P. Komm, N. Friedman, T. Eliash, M. Sheves, S. Ruhman, Deciphering excited state evolution in halorhodopsin with stimulated emission pumping, J. Phys. Chem. B 114 (2010) 3046–3051.
[33] S.L. Logunov, V.V. Volkov, M. Braun, M.A. El-Sayed, The relaxation dynamics of the excited electronic states of retinal in bacteriorhodopsin by two-pump-probe femtosecond studies, Proc. Natl. Acad. Sci. 98 (2001) 8475–8479.
[34] D. Polli, P. Altoe, O. Weingart, K.M. Spillane, C. Manzoni, D. Brida, G. Tomasello, G. Orlandi, P. Kukura, R.A. Mathies, M. Garavelli, G. Cerullo, Conical intersection dynamics of the primary photoisomerization event in vision, Nature 467 (2010) 440-U88.
[35] R.W. Schoenlein, L.A. Peteanu, Q. Wang, R.A. Mathies, C.V. Shank, Femtosecond dynamics of cis–trans isomerization in a visual pigment analog: isorhodopsin, J. Phys. Chem. 97 (1993) 12087–12092.
[36] A. Warshel, Bicycle-pedal model for the first step in the vision process, Nature (London) 260 (1976) 679.
[37] A. Warshel, N. Barboy, Energy storage and reaction pathways in the first step of the vision process, J. Am. Chem. Soc. 104 (1982) 1469–1476.
[38] A. Warshel, Z.T. Chu, J. Hwang, The dynamics of the primary event in rhodopsins revisited, Chem. Phys. 158 (1991) 303–314.
[39] A. Warshel, Z.T. Chu, Nature of the surface crossing process in bacteriorhodopsin: computer simulations of the quantum dynamics of the primary photochemical event, J. Phys. Chem. B 105 (2001) 9857–9871.
[40] R.S.H. Liu, A.E. Asato, The primary process of vision and the structure of bathorhodopsin: a mechanism for photoisomerization of polyenes, Proc. Natl. Acad. Sci. U. S. A. 82 (1985) 259–263.
[41] R.H. Liu, G. Hammond, The case of medium-dependent dual mechanisms for photoisomerization: one-bond-flip and hula-twist, Proc. Natl. Acad. Sci. U. S. A. 97 (2000) 11153–11158.
[42] R.S.H. Liu, Photoisomerization by hula-twist: a fundamental supramolecular photochemical reaction, Acc. Chem. Res. 34 (2001) 555–562.
[43] L.M. Frutos, T. Andruniow, F. Santoro, N. Ferre, M. Olivucci, Tracking the excited-state time evolution of the visual pigment with multiconfigurational quantum chemistry, Proc. Natl. Acad. Sci. U. S. A. 104 (2007) 7764–7769.
[44] P. Altoè, A. Cembran, M. Olivucci, M. Garavelli, Aborted double bicycle-pedal isomerization with hydrogen bond breaking is the primary event of bacteriorhodopsin proton pumping, Proc. Natl. Acad. Sci. U. S. A. 107 (2010) 20172–20177.
[45] J.J. Szymczak, M. Barbatti, H. Lischka, Is the photoinduced isomerization in retinal protonated Schiff bases a single- or double-torsional process? J. Phys. Chem. A 113 (2009) 11907–11918.
[46] S. Hayashi, E. Tajkhorshid, K. Schulten, Ab initio QM/MM molecular dynamics simulation of bacteriorhodopsin's photoisomerization using ab initio forces for the excited chromophore, Biophys. J. 85 (2003) 1440–1449.
[47] D.A. Case, D.A. Pearlman, J.W. Caldwell, T.E. Cheatham III, J. Wang, W.S. Ross, C.L. Simmerling, T.A. Darden, K.M. Merz, R.V. Stanton, A.L. Cheng, J.J. Vincent, M. Crowley, V. Tsui, H. Gohlke, R.J. Radmer, Y. Duan, J. Pitera, I. Massova, G.L. Seibel, U.C. Singh, P.K. Weiner, P.A. Kollman, AMBER. (2002) 7.
[48] U.F. Rohrig, L. Guidoni, A. Laio, I. Frank, U. Rothlisberger, A molecular spring for vision, J. Am. Chem. Soc. 126 (2004) 15328–15329.
[49] D.C. Teller, T. Okada, C.A. Behnke, K. Palczewski, R.E. Stenkamp, Advances in determination of a high-resolution three-dimensional structure of rhodopsin, a model of G-protein-coupled receptors (GPCRs), Biochemistry 40 (2001) 7761–7772.
[50] N. Ferre, A. Cembran, M. Garavelli, M. Olivucci, Complete-active-space self-consistent-field/Amber parameterization of the Lys296–retinal–Glu113 rhodopsin chromophore-counterion system, Theor. Chem. Acc. 112 (2004) 335–341.
[51] S. Hayashi, E. Taikhorshid, K. Schulten, Photochemical reaction dynamics of the primary event of vision studied by means of a hybrid molecular simulation, Biophys. J. 96 (2009) 403–416.
[52] I. Schapiro, O. Weingart, V. Buss, Bicycle-pedal isomerization in a rhodopsin chromophore model, J. Am. Chem. Soc. 131 (2009) 16–17.
[53] W.C. Chung, S. Nanbu, T. Ishida, QM/MM trajectory surface hopping approach to photoisomerization of rhodopsin and isorhodopsin: the origin of faster and more efficient isomerization for rhodopsin, J. Phys. Chem. B 116 (2012) 8009–8023.
[54] R.R. Birge, L.M. Hubbard, Molecular dynamics of trans–cis isomerization in bathorhodopsin, Biophys. J. 34 (1981) 517–534.
[55] I. Schapiro, M.N. Ryazantsev, L. Manuel Frutos, N. Ferre, R. Lindh, M. Olivucci, The ultrafast photoisomerizations of rhodopsin and bathorhodopsin are modulated by bond length alternation and HOOP driven electronic effects, J. Am. Chem. Soc. 133 (2011) 3354–3364.
[56] A.M. Virshup, C. Punwong, T.V. Pogorelov, B.A. Lindquist, C. Ko, T.J. Martínez, Photodynamics in complex environments: ab initio multiple spawning quantum mechanical/molecular mechanical dynamics, J. Phys. Chem. B 113 (2009) 3280–3291.
[57] K. Jung, V.D. Trivedi, J.L. Spudich, Demonstration of a sensory rhodopsin in eubacteria, Mol. Microbiol. 47 (2003) 1513–1522.
[58] O.A. Sineshchekov, E.N. Spudich, V.D. Trivedi, J.L. Spudich, Role of the cytoplasmic domain in Anabaena sensory rhodopsin photocycling: vectoriality of Schiff base deprotonation, Biophys. J. 91 (2006) 4519–4527.
[59] L. Vogeley, V.D. Trivedi, O.A. Sineshchekov, E.N. Spudich, J.L. Spudich, H. Luecke, Crystal structure of the Anabaena sensory rhodopsin transducer, J. Mol. Biol. 367 (2007) 741–751.
[60] M. Kondoh, K. Inoue, J. Sasaki, J.L. Spudich, M. Terazima, Transient dissociation of the transducer protein from anabaena sensory rhodopsin concomitant with formation of the M state produced upon photoactivation, J. Am. Chem. Soc. 133 (2011) 13406–13412.
[61] H. Irieda, T. Morita, K. Maki, M. Homma, H. Aiba, Y. Sudo, Photo-induced regulation of the chromatic adaptive gene expression by Anabaena sensory rhodopsin, J. Biol. Chem. 287 (2012) 32485–32493.
[62] L.S. Brown, Eubacterial rhodopsins — Unique photosensors and diverse ion pumps, Biochimica et Biophysica Acta (BBA) — Bioenergetics (2013), http://dx.doi.org/10.1016/j.bbabio.2013.05.006.
[63] A. Kawanabe, H. Kandori, Photoreactions and structural changes of Anabaena sensory rhodopsin, Sensors 9 (2009) 9741–9804.
[64] O.A. Sineshchekov, V.D. Trivedi, J. Sasaki, J.L. Spudich, Photochromicity of Anabaena sensory rhodopsin, an atypical microbial receptor with a cis-retinal light-adapted form, J. Biol. Chem. 280 (2005) 14663–14668.
[65] W. Stoeckenius, R.H. Lozier, R.A. Bogomolni, Bacteriorhodopsin and the purple membrane of halobacteria, Biochim. Biophys. Acta Bioenerg. 505 (1979) 215–278.
[66] P. Scherrer, M.K. Mathew, W. Sperling, W. Stoeckenius, Retinal isomer ratio in dark-adapted purple membrane and bacteriorhodopsin monomers, Biochemistry (N. Y.) 28 (1989) 829–834.
[67] A. Wand, R. Rozin, T. Eliash, K. Jung, M. Sheves, S. Ruhman, Asymmetric toggling of a natural photoswitch: ultrafast spectroscopy of Anabaena sensory rhodopsin, J. Am. Chem. Soc. 133 (2011) 20922–20932.
[68] A. Strambi, B. Durbeej, N. Ferré, M. Olivucci, Anabaena sensory rhodopsin is a light-driven unidirectional rotor, Proc. Natl. Acad. Sci. 107 (2010) 21322–21326.
[69] P.B. Coto, A. Strambi, N. Ferré, M. Olivucci, The color of rhodopsins at the ab initio multiconfigurational perturbation theory resolution, Proc. Natl. Acad. Sci. U. S. A. 103 (2006) 17154–17159.
[70] T. Andruniow, N. Ferre, M. Olivucci, Structure, initial excited-state relaxation, and energy storage of rhodopsin resolved at the multiconfigurational perturbation theory level, Proc. Natl. Acad. Sci. U. S. A. 101 (2004) 17908–17913.
[71] N. Ferré, M. Olivucci, Probing the rhodopsin cavity with reduced retinal models at the Caspt2//Casscf/Amber level of theory, J. Am. Chem. Soc. 125 (2003) 6868–6869.
[72] Andersson, K.; Aquilante, F.; Barysz, M.; Bednarz, E.; Bernhardsson, A.; Blomberg, M. R. A.; Carissan, Y.; Cooper, D. L.; Cossi, M.; Devarajan, A.; Vico, L. D.; Ferré, N.; Fülscher, M. P.; Gaenko, A.; Gagliardi, L.; Ghigo, G.; Graaf, C. d.; Hess, B. A.; Hagberg, D.; Holt, A.; Karlström, G.; Krogh, J. W.; Lindh, R.; Malmqvist, P.-.; Nakajima, T.; Neogrády, P.; Olsen, J.; Pedersen, T. B.; Raab, J.; Reiher, M.; Roos, B. O.; Ryde, U.;

Schimmelpfennig, B.; Schütz, M.; Seijo, L.; Serrano-Andrés, L.; Siegbahn, P. E. M.; Stålring, J.; Thorsteinsson, T.; Veryazov, V.; Widmark, P.-.; Wolf, A. Molcas. 2009, *version 7.4* http://molcas.org/.

[73] F. Aquilante, L. De Vico, N. Ferré, G. Ghigo, P. Malmqvist, P. Neogrády, T.B. Pedersen, M. Pito?ák, M. Reiher, B.O. Roos, L. Serrano-Andrés, M. Urban, V. Veryazov, R. Lindh, MOLCAS 7: the next generation, J. Comput. Chem. 31 (2010) 224–247.

[74] J.W. Ponder, F.M. Richards, Tinker molecular modeling package, J. Comp. Chem. 8 (1987) 1016–1024.

[75] A. Strambi, P.B. Coto, L.M. Frutos, N. Ferre, M. Olivucci, Relationship between the excited state relaxation paths of rhodopsin and isorhodopsin, J. Am. Chem. Soc. 130 (2008) 3382–3388.

[76] J. Stålring, A. Bernhardsson, R. Lindh, Analytical gradients of a state average MCSCF state and a state average diagnostic, Mol. Phys. 99 (2001) 103.

[77] L. Blancafort, F. Ogliaro, M. Olivucci, M.A. Robb, M.J. Bearpark, A. Sinicropi, Computational investigation of photochemical reaction mechanisms, in: A. Kutateladze (Ed.), Computational Methods in Photochemistry, Vol. 14, CRC Press, New York, 2005, pp. 31–110.

[78] G. Groenhof, M. Bouxin-Cademartory, B. Hess, S.P. de Visser, H.J.C. Berendsen, M. Olivucci, A.E. Mark, M.A. Robb, Photoactivation of the photoactive yellow protein: why photon absorption triggers a trans-to-cis isomerization of the chromophore in the protein, J. Am. Chem. Soc. 126 (2004) 4228–4233.

[79] L.V. Schäfer, G. Groenhof, M. Boggio-Pasqua, M.A. Robb, H. Grubmüller, Chromophore protonation state controls photoswitching of the fluoroprotein asFP595, PLoS Comput. Biol. 4 (2008) e1000034.

[80] Federico Melaccio, Nicolas Ferré, Massimo Olivucci, Phys. Chem. Chem. Phys. 14 (2012) 12485–12495.